Redefinition of the Amplitude Probability Distribution Measuring Function for Electromagnetic Emissions Assessment

Marc García Bermúdez[1], **Xileidys Parra**[2], **and Marco A. Azpúrua**[1, 2]

[1]Universitat Politècnica de Catalunya, Spain
[2]EMC Electromagnetic BCN, S.L., Spain

Abstract— The amplitude probability distribution (APD) is a measuring function for assessing electromagnetic disturbances, especially those with a stochastic and time-varying distribution. According to the CISPR 16-1-1, the APD has been defined as the cumulative distribution of the probability of time that the amplitude of disturbance exceeds a specified level. The APD is highly correlated to the bit error rate of digital communication systems, and therefore, a redefinition of radiated emission limits based on the APD would be very meaningful in terms of protecting wireless systems from unintentional interferences. However, establishing emissions requirements based on the current standard APD method can be misleading and not completely traceable metrology-wise. This is because, when analyzing electromagnetic compatibility (EMC) standards, the current specifications for APD measurements are unclear and ill-posed. For instance, the APD is only defined for applications above 1 GHz and with a fixed resolution bandwidth of 1 MHz; both conditions are arbitrarily set due to legacy considerations. Given the capabilities and flexibility of available instrumentation technology, we will propose an improved and more general APD definition accompanied by a calculation algorithm. Moreover, we argue that the APD measurements shall move from a histogram-based approach and implement kernel density estimation instead. We deliver evidence that exemplifies and supports our revised APD definition through numerical simulations. The study closes with a critical discussion about why the APD is so relevant and how it can be redefined to become widely employed as part of EMC assessments.

1. INTRODUCTION

Wireless systems play a crucial role in the progress of technology and society in modern times. Significant technological advancements such as smart cities, smart grid, autonomous vehicles, the Internet of Things (IoT), and others rely heavily on wireless systems [1, 2].

The likelihood of malfunctioning due to interferences is higher in a world increasingly dependent on wireless communications. On the one hand, the wireless coexistence problem is primarily encountered in the crowded ISM bands where numerous devices simultaneously transmit and receive large volumes of data over the air using high-throughput communications. Conversely, any electronic device produces unintentional radiofrequency emissions that may degrade the performance of wireless communication. This is electromagnetic interference (EMI) from the electromagnetic compatibility (EMC) standpoint.

Despite being a contemporary issue, EMC challenges have been a concern for a long time. It has been well-recognized that protecting wireless communication systems and their applications against radiated electromagnetic interference (EMI) is crucial [3]. In this regard, numerous EMC standards and recommendations exist from prominent organizations like IEC, IEEE, and ITU. These standards address the testing methods and requirements that electronic equipment must adhere to to ensure they do not disturb radiocommunication and other equipment when used as intended.

Over 80 years ago, the International Special Committee on Radio Interference (CISPR) was established to ensure consistent testing methods and requirements to minimize unintentional EMI. Despite the evolution of wireless systems from analog to complex digital systems, the methods for testing electric and electronic equipment's electromagnetic emissions have remained the same. In summary, the fundamental tool for assessing EMI is the measuring receiver, a standardized instrument designed to offer a consistent reading of the disturbance spectrum level through weighting detectors like the quasi-peak (QP) [4].

However, as our communications systems evolve, so must the reference methods used to assess and prevent EMI. It is, therefore, of prime relevance to ask ourselves whether existing interference measurement standards are adequate for our current and future needs in this area. For instance,

most wireless systems quantify transmission quality in terms of metrics like bit/frame error rate, packet loss, error vector magnitude and throughput, among others [1, 5]. Matsumoto and Wiklundh have extensively investigated digital radio systems and the evaluation of the interfering noise impact on them. They concluded the Amplitude Probability Distribution (APD) of a signal is one of the statistical properties of random signals that can be used to determine the capability of a device to generate interference in digital communication systems [6–8]. This affirmation has been confirmed due to the high correlation between the APD measurements of disturbances and the bit error rate (BER) as a quality degradation index for victim systems. Conversely, standard EMI testing using the QP detector can hardly be used to predict real EMI problems [9].

The above-cited research has slightly permeated EMC standards. In particular, in the CISPR 16-1-1:2019, we can find the standard definition of the APD and a set of requirements and specifications for it as a complementary measuring function of the test receiver. In that sense, the standard defines the APD of a disturbance as the cumulative distribution of the "probability of time that the amplitude of disturbance exceeds a specified level" [4]. However, the usefulness of the standard APD measuring function is diminished due to the self-imposed limitations given in the said standard's clauses. Firstly, the frequencies for which the APD is expected to be measured are restricted from 1GHz to 18GHz. Secondly, the measurement bandwidth required by the standard is fixed to 1 MHz and not to the bandwidth of the communication channel. Third, the frequentist approach to probability used in the calculation algorithm required collecting a massive number of samples to reach probability levels as low as 10^{-7}, resulting in slow measurements. Finally, no well-established standard limits can be used to determine compliance during emissions testing using APD.

Therefore, EMC standards must be revised to improve the APD definition and to favour its application as part of EMI measurements. In the next sections, we will describe and argue the changes to fix the limitations identified in the standard. The structure of the paper is as follows: Section 2 reviews the fundamental concepts of the APD in the EMC context. Then, Section 3 summarizes the aspects of the standard APD measuring function and Section 4 deals with the generalized APD definition. Afterwards, numerical experiments are provided to support and exemplify the improvements achieved with the redefined APD measuring function. The article closes with some final remarks and conclusions in Section 5.2.

2. APD FUNDAMENTALS

Considering a signal $x(t)$, the APD function, $APD(x_{th})$, returns the probability that an instantaneous amplitude of its envelope of a signal, $x_{env}(t)$, is greater than a previously specified threshold, x_{th}, that is,

$$APD(x_{th}) = P(x_{env}(t) > x_{th}). \tag{1}$$

where $x_{env}(t)$ is obtained through the in-phase and quadrature components of the down-converted signal, $x_i(t)$ and $x_q(t)$, respectively,

$$x_{env}(t) = \sqrt{x_I^2(t) + x_Q^2(t)}. \tag{2}$$

In other words, the APD function quantifies the time the measured envelope of an interfering signal exceeds a certain level [10].

If X_{env} is defined as a random variable of amplitudes (x) with a probability density function (pdf), $f_{X_{env}}(x)$, distributed according to the instantaneous values of $x_{env}(t)$, then the APD of X_{env}, $APD_{X_{env}}(x)$ is defined as,

$$APD_{X_{env}}(x) = 1 - F_{X_{env}}(x) \tag{3}$$

where $F_{X_{env}}(x)$ is the cumulative distribution function (cdf) of X_{env}. That is,

$$f_{X_{env}} = \frac{dF_{X_{env}}(x)}{dx}. \tag{4}$$

This fundamental definition means that measuring the APD requires estimating the $f_{X_{env}}(x)$ of the electromagnetic emissions. The most basic method for doing such estimation is the histogram of relative frequencies as explained in [11]. Other more complex and powerful approaches exist, including Kernel Density Estimation (KDE), as recommended in Section 4. However, if we stick with the histogram approach, then two different implementations are commonly reported:

- **Using comparators and counters** to determine the probabilities of exceeding a set of pre-assigned amplitude levels. The number of comparators equals the number of levels. This implementation is not that flexible and is not employed most of the time.
- **Employing an analog-to-digital converter (ADC)**, a logic circuit and a memory block. This is the most common approach.

For the sake of clarity and flexibility, we focused on the latter method. As a summary, Fig. 1 shows a block diagram of the fundamental APD calculation process. Here, the radiofrequency input is progressively transformed until the signal envelope is extracted and converted to the digital domain, where all the statistical processing is performed for measuring the APD.

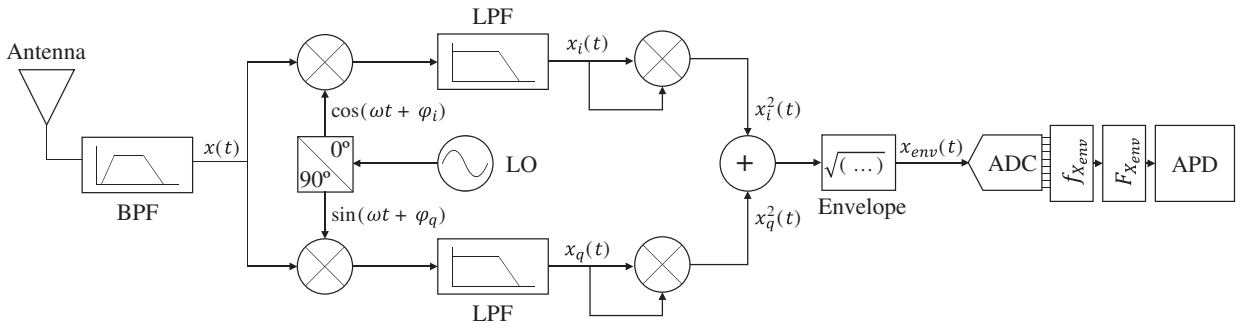

Figure 1: General block diagram of the APD measuring function.

Finally, it is important to remark that APD measurements are displayed in a graph where the signal amplitude thresholds are distributed along the horizontal axis in decibel units. In contrast, the probability of the signal amplitude exceeding the specified level is depicted in the vertical axis. If the histogram method is used, then the maximum number of levels at which APD is calculated is limited by the resolution of the receiver's ADC. Consequently, the span of the horizontal axis is linked to the dynamic range of the measuring instrument. On the other hand, the vertical axis usually presents probabilities as low as 10^{-7}. We must remember that accurately estimating such low probabilities using the histogram method requires enormous data sets. Hence, the lower bound of the vertical range in the APD graph is directly related to the sampling rate, the measurement time (observation window) and the total memory of the measurement device.

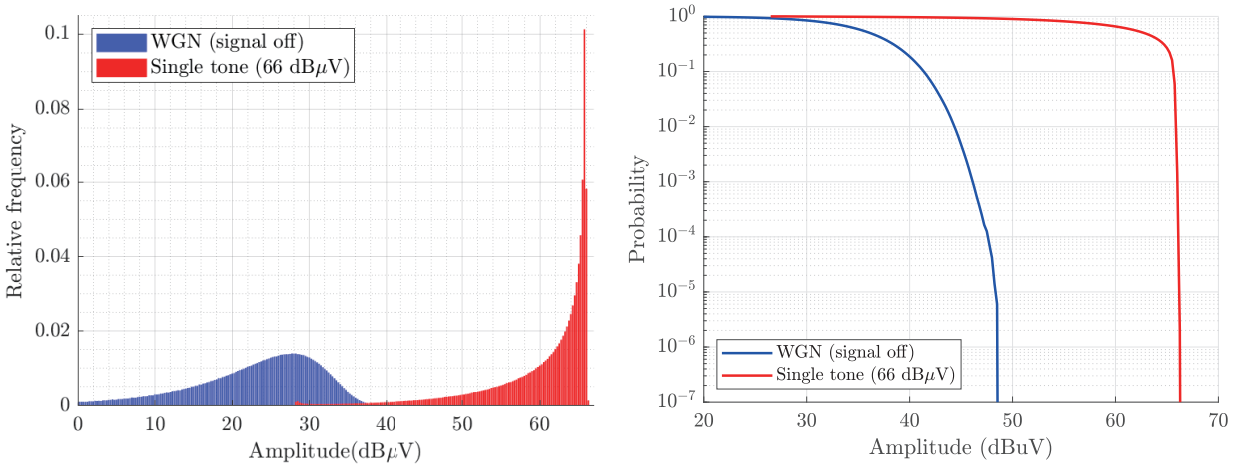

(a) Histogram (b) APD

Figure 2: Example of the APD graph for synthesized waveforms: White Gaussian Noise (Blue) and Narrow-band signal (Red).

3. THE STANDARD APD MEASURING FUNCTION

The latest CISPR 16-1-1 includes a clause about "Measuring receivers for the frequency range 1 GHz to 18 GHz with amplitude probability distribution (APD) measuring function" and also the

informative Annex G "Rationale for the specifications of the APD measuring function". In this section, we analyze that document and identify the handicaps it has.

- **The frequency range** is restricted above 1 GHz. However, in a note, the standard also says, "APD measurements can also be applicable in the frequency range below 1 GHz". Still, none of the specifications is coherent with the possibility of using APD measuring function below 1 GHz, as everything is referred to the resolution bandwidth used in the CISPR band E, which is 1 MHz.
- **The dynamic range of the amplitude** is defined as the level range necessary to obtain an APD that complies with the standards. The upper limit shall be greater than the peak level of disturbance to be measured, and the lower limit shall be lower than the level of disturbance limit specified by the product committees. This already convoluted specification is derived from a compromise value of 60 dB that was decided considering the emissions limits in the CISPR 11 [12]. In particular, according to the said standard, products belonging to Group 2 and which are also Class B have a peak limit set at 110 dBµV and a weighted limit specified at 60 dBμV. Therefore, a dynamic range of at least 60 dB is defined by adding a 10 dB of margin.
- **The tolerance in the level accuracy** shall be better than ± 2.7 dB in total. This is a substantial interval, therefore allowing for large measurement uncertainties. Moreover, its rationale is not explained in the corresponding standard. This specification should have been based on a complete measurement uncertainty analysis for the APD function. Unfortunately, this is not presented in the standard.
- **The maximum measurable time** of a disturbance shall be longer than or equal to 2 min. It is allowed to perform intermittent measurements if the blind time is less than 1% of the total measurement time. Such measurement time is based on the CISPR 11 requirement for microwave cooking appliances above 1 GHz. However, the said standard also recognizes the time requirements pose a challenge regarding memory. Again, this criterion is ill-defined. The suitable measurement time should be decided for each product according to the time-varying behaviour of electromagnetic emissions. For instance, if the dynamics of the disturbance and its repetition frequency are known (i.e. switching frequency, clock frequency, operating mode cycle duration, etc.), the measurement time can be fitted to whatever is sufficient for the APD.
- **The minimum measurable probability** shall be 10^{-7}. According to the CISPR 16-1-1, "about 100 occurrences might be necessary to obtain a meaningful result". Therefore, in the standard, this probability of 10^{-7} is approximately calculated as 100 bin counts divided by the total number of sample points captured during 120 s at a 10 MSa/s sampling rate. Again, this requirement has little statistical rigour, relies on the frequentist approach to probability, and is based on arbitrary assumptions about the measurement time, sampling rate and the distribution of the amplitudes.
- **The display resolution** of the APD measurement data shall be 0.25 dB or better. In CISPR 16-1-1, this figure is said to be obtained by dividing the required dynamic range of the amplitude (60 dB) by the number of discrete quantized levels of an 8-bit ADC (256). Again, this justification is poorly funded as ADCs are typically linear; otherwise, a logarithmic ADC assumption should have been stated.
- **The sampling rate** shall be greater than or equal to 10 MSa/s when using a resolution bandwidth of 1 MHz. There are two problems with this requirement: First, the standard requires a measurement bandwidth that could be different from the one of the radio service to be protected. Second, considering the signal envelope is already filtered to the required bandwidth, sampling it at five times the Nyquist rate doesn't provide further information. It is considered that the sampling rate requirement could be relaxed without the risk of aliasing errors.

4. GENERALIZED APD MEASURING FUNCTION

Figure 3 presents the block diagram of the redefined and generalized APD measurement function. Each processing step will be described in what follows, from signal acquisition to results display.

This proposal is based on direct-sampling techniques, as those employed in CISPR-compliant Full Time Domain EMI measurement systems [13–18]. The continuous waveform $x(t)$ is sampled

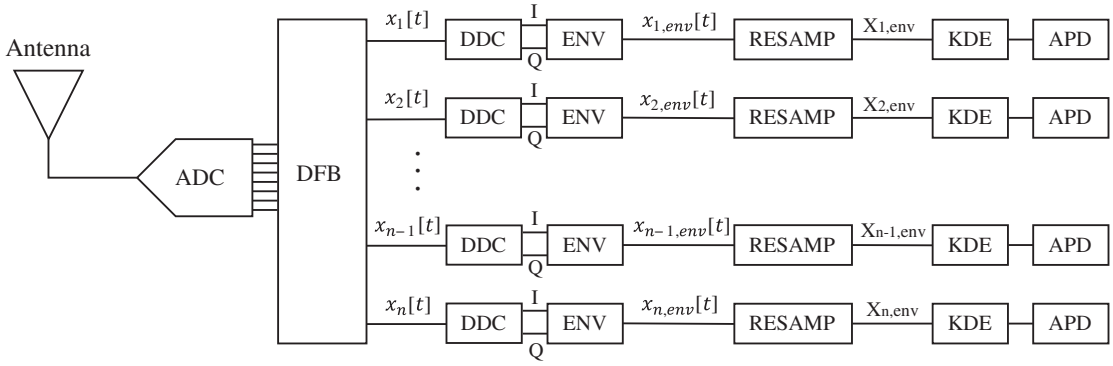

Figure 3: Block diagram of the redefined APD measuring function for a received signal.

at full bandwidth using high-resolution ADCs. Then, a digital filter bank (DFB) decomposes the digitized input $x[t]$, into n parallel signals, $x_k[t]$ for $k = 1, 2, \ldots n$, each one characterized by a bandwidth and centre frequency selected according to the specifications of the wireless system to be protected. Afterwards, digital down conversion (DDC) is performed to extract the I/Q components in baseband. The I/Q components are subsequently employed to calculate the corresponding envelope, $x_{k,env}[t]$. Next, the k-th envelope is resampled, and the resulting samples are used to find the envelope pdf using the Kernel Density Estimation (KDE) method. Ultimately, the APD is calculated at any amplitude level.

Regarding the envelope resampling block, we propose using a nonuniform scheme, interpolating the envelope amplitude at N randomised time instants [19]. This is important because it allows for extracting more information regarding the amplitude distribution of the envelope and reduces unwanted correlations due to repetitive points and periodicity effects. Such randomization can be obtained by adding a controlled jitter to a uniformly spaced time vector, that is,

$$\mathbf{t}_{rs} = \mathbf{t} + \tau \tag{5}$$

where $\mathbf{t} = \{t_1, t_1 + \Delta t, t_1 + 2\Delta t, \ldots, t_1 + N\Delta t\}$ is a set of exact time instants for each envelope point produced at a regular period, Δt, and $\tau = \{\tau_1, \tau_2, \ldots, \tau_N\}$ is the additive jitter randomly generated within the $\pm\Delta t/2$ interval for each envelope point. For performing the envelope interpolation, the modified Akima algorithm is recommended [20].

The output of the resampling block is a set of envelope amplitude values $\mathbf{X_{k,env}} = \{X_{(k,env),1}, X_{(k,env),2}, \ldots, X_{(k,env),N}\}$. The distribution of $X_{k,env}$ is unknown, but it can be estimated using $\mathbf{X_{k,env}}$ through the occurrences of the random variable $X_{k,env}$. Instead of using the histogram method, we recommend the KDE approach. The KDE is a non-parametric statistical technique used to estimate the pdf of a continuous random variable. The core idea of KDE is to estimate the density of a random variable by placing a "kernel" function at each data point and then summing these kernel functions to obtain an estimate of the pdf, as given in (6). The kernel function is usually a smooth, symmetric probability density function, such as the Gaussian or Epanechnikov kernel, which is centred at each data point and smoothed according to the parameter h, which determines how wide or narrow the kernel is.

$$\hat{f}_{k,env}(x) = \frac{1}{Nh} \sum_{j=1}^{N} K\left(\frac{X_{k,env} - X_{(k,env),j}}{h}\right) \tag{6}$$

Afterwards, the cdf is evaluated at certain amplitude threshold values, $x_{k,th}$, as

$$F_{k,env}(x_{k,th}) = \int_{-\infty}^{x_{k,th}} \hat{f}_{k,env}(x)dx, \tag{7}$$

where $x_{k,th}$ should be evenly distributed using a bin width calculated using a statistical criterion and within a range that allows reaching the required probability levels. For instance, Scott's rule is often a good rule of thumb in this regard [21]. Finally, $F_{k,env}(x_{k,th})$ is inputted into (3) for obtaining $APD_{X_{k,env}}(x_{k,th})$.

5. RESULTS

5.1. Experiment 1: APD for a Reduced Number of Sampled Waveform Points

One of our main hypotheses when proposing this redefinition of the APD processing algorithm is that by using non-frequentist probabilistic methods, we could significantly reduce the required number of samples. This means reducing the measurement times while retaining equivalent results would be possible. Fig. 4 shows the APD measurements for different sampling frequencies and dwell times, as indicated in the captions. The input to the APD measurement functions is White Gaussian Noise (WGN), and the waveforms were generated using the sampling frequency, f_s, and dwell times, t_{dwell} indicated in Fig. 4 captions.

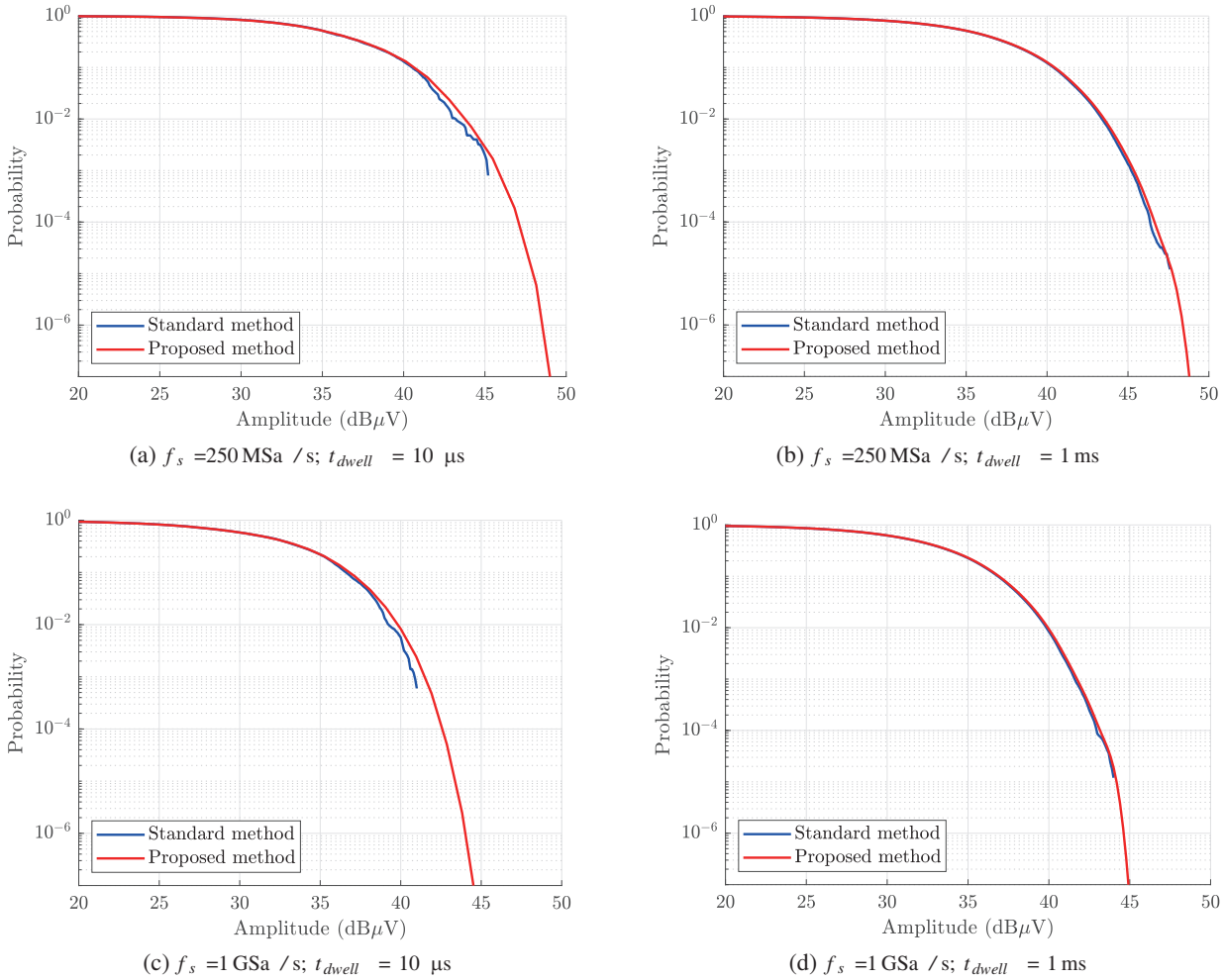

(a) f_s =250 MSa / s; t_{dwell} = 10 µs

(b) f_s =250 MSa / s; t_{dwell} = 1 ms

(c) f_s =1 GSa / s; t_{dwell} = 10 µs

(d) f_s =1 GSa / s; t_{dwell} = 1 ms

Figure 4: APD standard and proposed method comparison for different f_s and t_{dwell}.

As we can see, the standard APD algorithm can't estimate low probability levels under such a low number of input samples. Therefore, it does not deliver probabilities less than or equal to 10^{-7} for any reported cases. However, the proposed method can extrapolate lower probability levels with high accuracy. For this experiment, a Normal kernel has been selected. Whenever possible, the kernel selection can be made based on prior information about the distribution of the measurements.

On the other hand, the proposed APD does not vary significantly with the sampling time, but it does with the sampling frequency as does the standard APD. This might be related to the effective cutoff frequency of the finite impulse response (FIR) filter and how this depends on the signal sampling rate.

5.2. Experiment 2: APD for Multiple Resolution Bandwidth

Our second hypothesis is that the proposed APD measurement could be used to measure the interference level according to different channel bandwidths using the same measured sample, thus

reducing the total duration of APD measurements. Fig. 5 shows two APD graphs at different bandwidths for a sample of WGN and time-gated WGN, respectively.

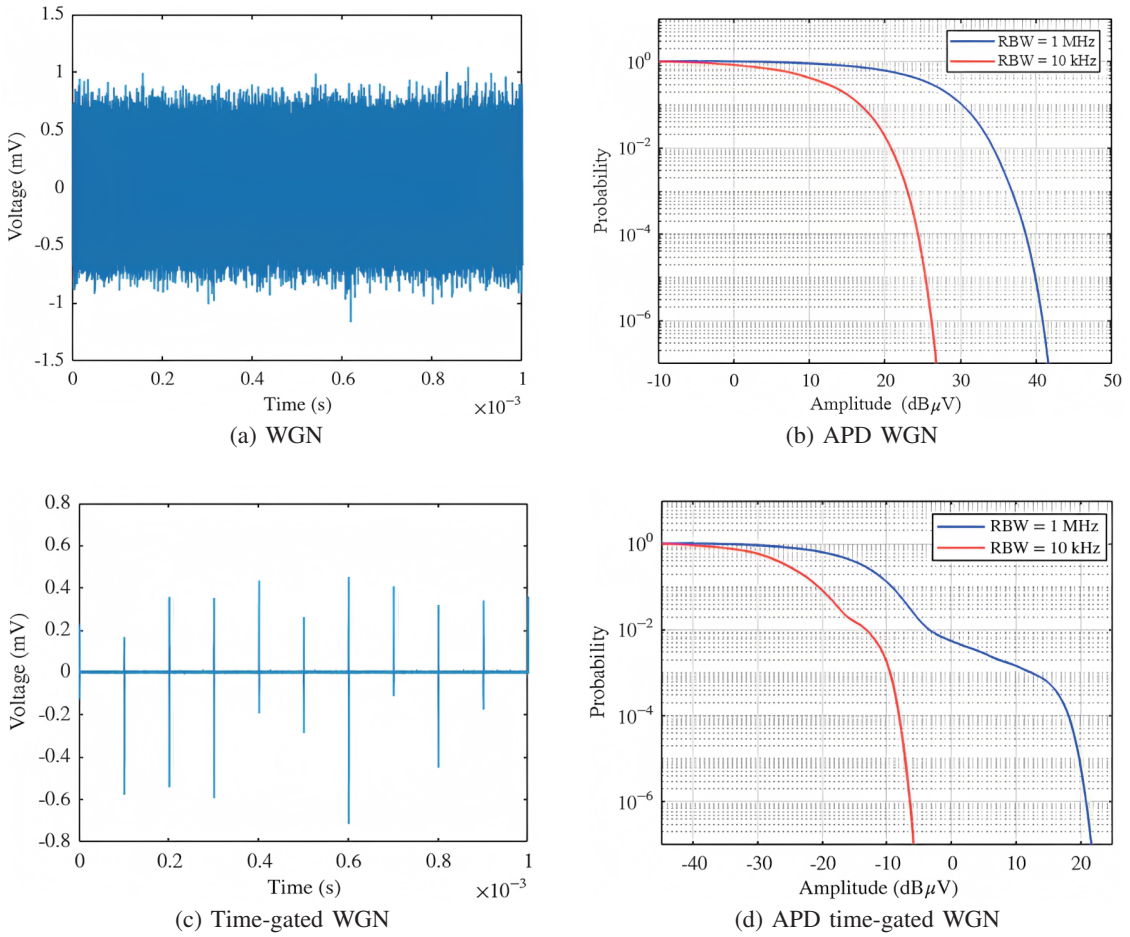

(a) WGN (b) APD WGN

(c) Time-gated WGN (d) APD time-gated WGN

Figure 5: APD standard and proposed method comparison for different resolution bandwidth.

As displayed in the results above, by filtering the signal to obtain different resolutions, we get the APD for the bandwidth of each channel, in this case, 1 MHz and 10 kHz.

6. CONCLUSION

This paper gives a more flexible and general definition for the APD measuring function, offering relevant advantages compared to the standard method. This has been briefly highlighted through a couple of numerical experiments. To conclude, a summary of the benefits and the aspects that must be further improved in our APD proposal is given.

First, this definition avoids unsubstantiated specifications or conditions currently identified in the standard APD measuring function. Also, the proposed method aligns with the core purpose of APD since it considers and handles the measured amplitude as a random variable. Therefore, our approach allows obtaining significant APD estimations using smaller samples, that is, in less measurement time. Under the same conditions, our algorithm delivers low probability levels that the standard procedure fails to detect. This is possible because of the application of KDE instead of the histogram method.

Secondly, the other fundamental improvement is that due to the combination of ultra-broadband measurements and digital filter banks, it is possible to calculate the APD for any required frequency range, adjusting the resolution bandwidth to the wireless system characteristic and making APD measurements more representative of the received noise/interference. This is potentially useful when establishing the interference impact on the quality of wireless communications and setting realistic electromagnetic emissions requirements. Moreover, this capability also shortens the overall testing time of APD-based EMC assessments.

Thirdly, given the all-digital nature of the new APD implementation, it does not require a specific measuring instrument to be obtained. This also means all parameters of the APD algorithm can be tuned to obtain better results, for example, selecting the most appropriate kernel function or configuring the exact filter characteristics of the receiver.

Concerning the filter bandwidths, even though they can be arbitrarily configured, to improve repeatability, it is advisable to define standard filter masks for each communication system to be protected. This would prevent any divergence due to a variation in the filter type or its coefficients.

This contribution to the APD definition can potentially improve EMI testing and evaluation, facilitating the procedures and reducing the measurement times to perform APD measures.

ACKNOWLEDGMENT

The project (21NRM06 EMC-STD) has received funding from the European Partnership on Metrology, co-financed by the European Union's Horizon Europe Research and Innovation Programme and by the Participating States.

EMC Barcelona's project under grant number SNEO-20211223 has received funding from CDTI, which is supported by "Ministerio de Ciencia e Innovación" and financed by the European Union — NextGenerationEU — through the guidelines included in the 'Plan de Recuperación, Transformación y Resiliencia".

Dr. Azpúrua has received funding from the StandICT.eu 2023 project, financed by the European Union's Horizon Europe — Research and Innovation Programme — under grant agreement No. 951972.

REFERENCES

1. Pous, M., M. A. Azpúrua, and F. Silva, "Improved electromagnetic compatibility standards for the interconnected wireless world," *2019 International Symposium on Electromagnetic Compatibility — EMC EUROPE*, 1055–1060, 2019.
2. Mynster, A. P. and P. T. Jensen, "Emc for the iot," *2016 International Symposium on Electromagnetic Compatibility — EMC EUROPE*, 144–149, 2016.
3. *Directive 2014/30/EU of the European Parliament and of the Council of 26 February 2014 on the harmonisation of the laws of the Member States relating to electromagnetic compatibility (recast) Text with EEA relevance.*
4. "CISPR 16-1-1:2019 Ed 5.0. Specification for radio disturbance and immunity measuring apparatus and methods — Part 1-1: Radio disturbance and immunity measuring apparatus — Measuring apparatus," IEC, Geneva, CH, Standard, Jun. 2019.
5. Pous, M., M. A. Azpúrua, and F. Silva, "Measurement and evaluation techniques to estimate the degradation produced by the radiated transients interference to the gsm system," *IEEE Transactions on Electromagnetic Compatibility*, Vol. 57, No. 6, 1382–1390, 2015.
6. Matsumoto, Y. and K. Gotoh, "An expression for maximum bit error probability using the amplitude probability distribution of an interfering signal and its application to emission requirements," *IEEE Transactions on Electromagnetic Compatibility*, Vol. 55, No. 5, 983–986, 2013.
7. Matsumoto, Y., "On the relation between the amplitude probability distribution of noise and bit error probability," *IEEE Transactions on Electromagnetic Compatibility*, Vol. 49, No. 4, 940–941, 2007.
8. Wiklundh, K., "Relation between the amplitude probability distribution of an interfering signal and its impact on digital radio receivers," *IEEE Transactions on Electromagnetic Compatibility*, Vol. 48, No. 3, 537–544, 2006.
9. Pous, M., "Radiated transient interferences in digital communication systems," Ph.D. dissertation, Barcelona, Spain, 2015.
10. Stenumgaard, P., "Using the root-mean-square detector for weighting of disturbances according to its effect on digital communication services," *IEEE Transactions on Electromagnetic Compatibility*, Vol. 42, No. 4, 368–375, 2000.
11. Kim, H. and H. Sawada, "Histogram meets topic model: Density estimation by mixture of histograms," 2015.
12. "CISPR 11 Ed. 5: Industrial, scientific and medical equipment — Radio-frequency disturbance characteristics — Limits and methods of measurement," Comité International Spécial des Perturbations Radioélectriques, Geneva, CH, Standard, 2009.

13. Azpúrua, M. A., M. Pous, S. Çakir, M. Çetinta, and F. Silva, "Improving time-domain emi measurements through digital signal processing," *IEEE Electromagnetic Compatibility Magazine*, Vol. 4, No. 2, 82–91, 2015.
14. Azpúrua, M. A., M. Pous, and F. Silva, "A measurement system for radiated transient electromagnetic interference based on general purpose instruments," *2015 IEEE International Symposium on Electromagnetic Compatibility (EMC)*, 1189–1194, 2015.
15. Azpúrua, M. A., M. Pous, J. A. Oliva, B. Pinter, M. Hudlička, and F. Silva, "Waveform approach for assessing conformity of cispr 16-1-1 measuring receivers," *IEEE Transactions on Instrumentation and Measurement*, Vol. 67, No. 5, 1187–1198, 2018.
16. Azpúrua, M. A., M. Pous, M. Fernandez, and F. Silva, "Dynamic performance evaluation of full time domain emi measurement systems," *2018 International Symposium on Electromagnetic Compatibility (EMC EUROPE)*, 561–566, 2018.
17. Azpúrua, M. A., M. Pous, and F. Silva, "Specifying the waveforms for the calibration of cispr 16-1-1 measuring receivers," *IEEE Transactions on Electromagnetic Compatibility*, Vol. 62, No. 3, 654–662, 2020.
18. Azpúrua, M. A., M. Pous, and F. Silva, "Statistical evaluation of measurement accuracy in full time-domain emi measurement systems," *2020 International Symposium on Electromagnetic Compatibility — EMC EUROPE*, 1–6, 2020.
19. Martínez-Nuevo, P., "Nonuniform sampling rate conversion:an efficient approach," *IEEE Transactions on Signal Processing*, Vol. 69, 2913–2922, 2021.
20. Akima, H., "A new method of interpolation and smooth curve fitting based on local procedures," *J. ACM*, Vol. 17, No. 4, 589–602, Oct. 1970, [Online]. Available: https://doi.org/10.1145/321607.321609.
21. Scott, D. W., *Multivariate Density Estimation: Theory, Practice, and Visualization*, John Wiley, New York, 1992.